

## Possibilities of Using Impedance Spectroscopy for Indirect Measurements of Thin Layers of Al & Cr-Al Coatings on Ni-based Superalloy Inconel 713LC Applied by the "Out-of-pack" Diffusion Method

Michal Krbata (0000-0002-0520-8180), Peter Fabo (0000-0001-8370-3999), Marcel Kohutiar (0000-0002-4710-5913), Jana Escherova (0000-0002-4203-2495), Michal Kuba (0000-0002-8334-0515), Marta Kianicova (0000-0001-9083-9552), Maros Eckert (0000-0002-1266-8230), Faculty of Special Technology, Alexander Dubcek University of Trenčín, Ku Kyselke 469, 911 06 Trenčín, Slovakia. E-mail: marcel.kohutiar@tnuni.sk

The presented work deals with the research of the super-alloy Inconel 713LC, on which an Al-based coating was applied using the "Out-of-pack" diffusion coating process, or CrAl. In this contribution, the results of measuring the thickness of thin coatings using a confocal laser microscope and the method of impedance spectroscopy are presented and discussed. This can demonstrate the possibility of being used also for researching the properties of thin layers using a VF probe, which, thanks to the use of ferrite, has a practically constant inductance in the entire frequency range, and the presence of a metal sample in the magnetic circuit of the probe was manifested as a result of eddy currents by a significant decrease in the inductance value at higher frequencies. However, the measurements require precise measurement of impedance with an accuracy of  $1\text{m}\Omega$  and phase angle with an accuracy of  $0.001^\circ$  with high stability of the measuring frequency. For a better assessment of the parameters of the layers, it is necessary to extend the frequency range of the measurement to the range of MHz units.

**Keywords:** Coating, Layer thickness, Inconel, Impedance spectroscopy, Microstructure

### 1 Introduction

Nickel-based super alloys have been widely used in the energy industry for a long time. Their high-temperature properties, especially their high strength and toughness, high temperature stability, and environmental resistance made them a material particularly suitable for turbine blades, discs, and valves [1]. Degradation processes during maintenance regimes often determine the life of the turbine blade. In addition to damage caused by creep, the extreme environment of modern aircraft, terrestrial and marine engines affect the life of high temperature components. Despite the extraordinary oxidation and corrosion resistance of the Inconel 713LC [2], the surface must be protected from environmental effects [3,4] from high gases, including air and gases from combustion fuels, as operating temperatures in turbine engines increase. To provide sufficient corrosion and oxidation resistance at high temperatures, nickel-based superalloy components are often protected by diffusion coatings [5–11], although there is also great interest in overlay and TBC coatings [12–18]. The surface of the substrate is enriched by the diffusion reaction with aluminum. The increase in aluminum content in the vicinity of the surface supports the ability to form an aluminum ( $\text{Al}_2\text{O}_3$ ) protective scale and therefore improves oxidation and corrosion resistance. Specific coating properties are

often improved and modified by adding other elements such as Cr, Pt, and Si [19–22]. Chromium-modified aluminum diffusion coatings, among others, offer very effective thermal corrosion protection for nickel-based superalloys. In addition, Al-Cr diffusion coatings can be successfully applied up to  $1000^\circ\text{C}$  [23]. Since these components operate under demanding working conditions (high temperatures and temperature gradients, aggressive environments, thermal shocks), protective coatings are usually applied to protect the underlying substrate from the high-temperature degradation. In general, there are two types of coatings: bond coating (diffusion and overlay coating) and modern thermal barrier coating systems consisting of bond coating and insulating ceramic surface layers, which through active air cooling can reduce the substrate temperature to more than  $300^\circ\text{C}$  for the most exposed components [24–28].

Diffusion binder coatings are produced by increasing the aluminum content of the substrate through diffusion reactions. The high concentration of aluminum near the surface increases the ability to form a protective layer of aluminum oxide ( $\text{Al}_2\text{O}_3$ ), which provides resistance to corrosion and oxidation. Other elements such as Cr, Pt, Si, and Ti are often added to change the specific properties of coatings and improve their performance. In particular, it has

been shown that the addition of chromium provides the most effective protection against hot corrosion in nickel alloys [27, 28]. In addition to the corrosion of the chemically aggressive environment caused by heat corrosion, the turbine is exposed to significant stresses and deformations caused mainly by centrifugal and aerodynamic forces, vibration, and thermomechanical cycles [28].

The presented work investigates the possibilities of using impedance spectroscopy as an indirect method for measuring the thicknesses of thin coatings on the Inconel 713LC superalloy, on which an Al or CrAl-based coating was applied using "Out-of pack" diffusion coating. A LEXT OLS 5100 confocal laser microscope was used to control the direct measurement method.

**Tab. 3** Chemical composition of Inconel 713LC (wt.%)

Cr	Al	Mo	Nb	Ti	Zr	C	B	P	S	Ni
11.85	5.8	4.54	2.27	0.72	0.11	0.04	0.015	0.006	0.004	Balance

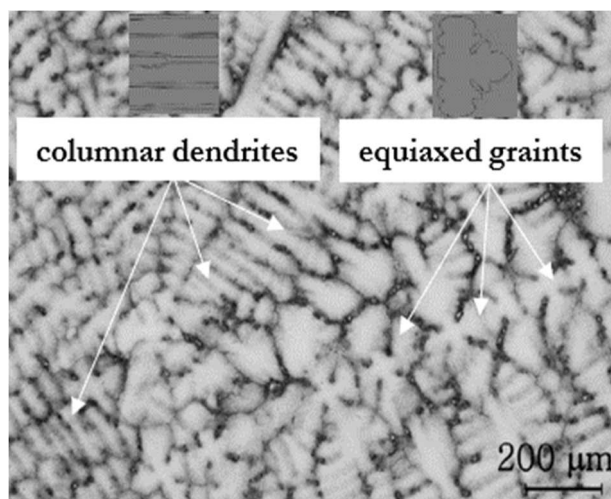


**Fig. 1** Macrostructure of Inconel 713LC [2]

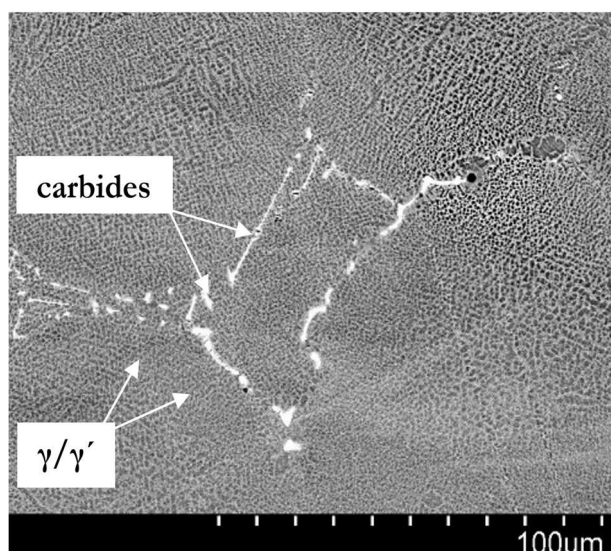


**Fig. 2** Microstructure of Inconel 713LC

## 2 Materials and methods

The experimental samples were made from coated Inconel 713LC rods [31]. The exact chemical composition of the Inconel 713LC base alloy was evaluated using the SPECTROMAXx emission spectrometer and is shown in Tab. 1. Macroscopic examination of the castings of Inconel 713LC material revealed a dendritic structure (Fig. 1), which consisted of columnar dendrites and equiaxed grains. The microstructure is typical of a cast Ni-based superalloy and consists of a  $\gamma$ -matrix, a strengthening phase  $\gamma'$  (cuboidal  $\text{Ni}_3(\text{Al}, \text{Ti})$  coherent precipitates) and primary MC carbides (Fig. 2).

The inductance measurements of the probe were carried out on the basic base metal (IN713LC) and on the surface with the implementation of thin layers (IN713LC + Al; IN713LC + CrAl). The measurement was carried out with an RLCG bridge and the working frequency range was 100-200 kHz according to the device setting at a voltage of 1 V. The measuring probe was made from a ferrite ring, which was cut with a diamond saw. 15 turns of HF wire were wound on the ferrite half-ring. In order to stabilize the device after switching on and during its use, a control measurement of the probe's own parameters was carried out before each measurement without the presence of the measured ones samples (designation "air").

## 3 Results and discussion

The interface between the outer species and the diffusion zone is well defined especially in the case of the IN713LC + Al sample (Fig. 3), while in the case of the IN713LC + CrAl sample (Fig. 4), the interface is more difficult to recognize due to the supersaturation of the diffusion zone and outer Cr layer [2]. The thickness of both types of samples was 5 mm. The measurement of the thickness of the layers [29, 30] was carried out on the device CLM LEXT OLS 5100. The total thickness of the layer on the sample IN713LC + Al reached the value of 58.382  $\mu\text{m}$ , while the ratio of the outer layer and the diffusion zone was approximately the same. On the IN713LC + CrAl sample, a significantly thicker outer layer compared to the diffusion zone was observed in a ratio of 4:1. The total thickness of the layer in the given sample was 75.709  $\mu\text{m}$ .

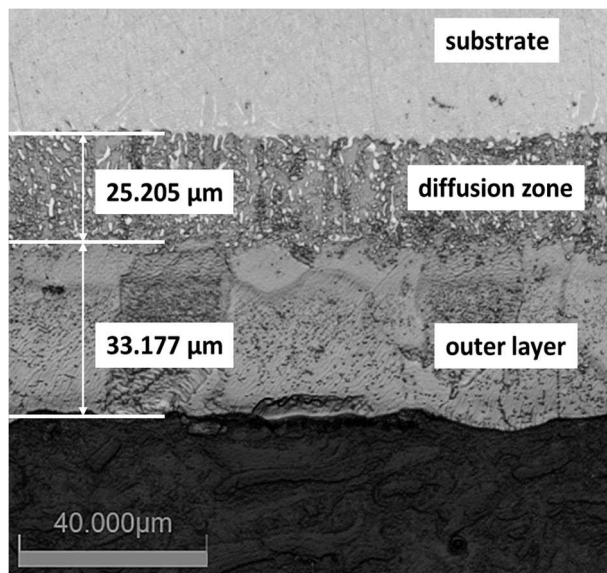


**Fig. 3** Thickness of layers of Inconel 713LC + Al

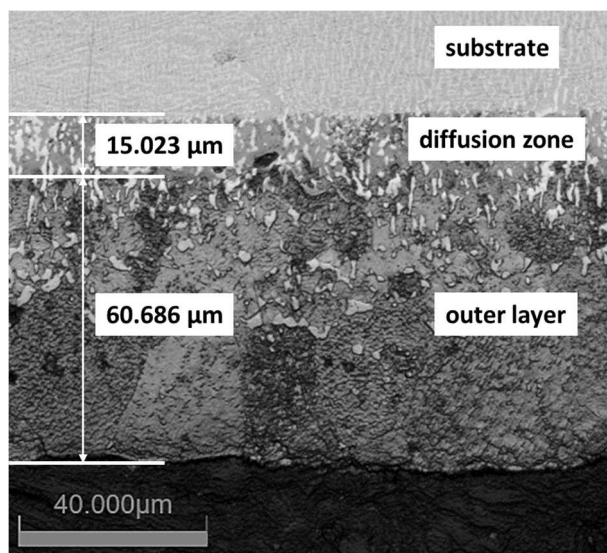


**Fig. 4** Thickness of layers of Inconel 713LC + CrAl

Evaluation of the microhardness of the base superalloy Inconel 713LC as well as its diffusion zones and outer layers, which are based on Al, or CrAl were evaluated on a QATM Qness 10 CHD MASTER+ device. When measuring the microhardness, the Vickers method was used with HV0.1 load. The microhardness of the base super-alloy Inconel 713LC had a value of 382 HV0.1. In the Inconel 713LC + Al sample (Fig. 5), the diffusion zone microhardness value increased to 562 HV0.1. The increase in hardness is caused by a combination of two factors. The first is the growth and spheroidization of the  $\gamma'$  phase, and the second is the dissolution of primary carbides and the precipitation of secondary carbides in the grain boundaries of the  $\gamma$  phase [32]. The Inconel 713LC + CrAl sample (Fig. 6) reached a microhardness of 514 HV0.1 in the diffusion zone, and the microhardness increased to 689 HV0.1 in the outer layers.

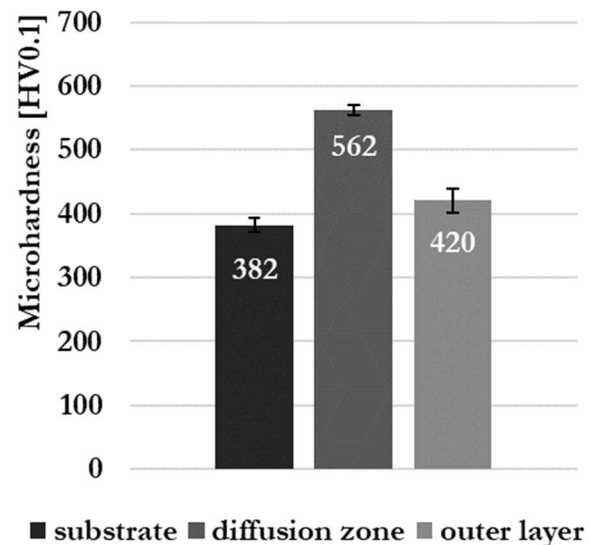


**Fig. 5** Microhardness of layers of Inconel 713LC + Al

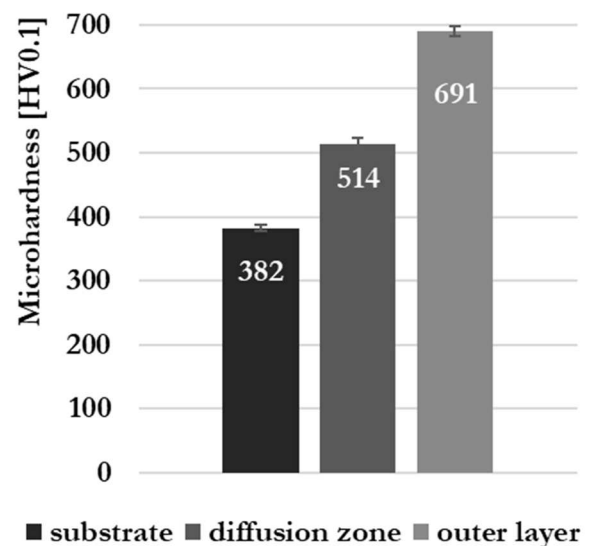


**Fig. 6** Microhardness of layers of Inconel 713LC + CrAl

A control measurement without the use of samples labeled "air" (Fig. 7 and Fig. 8) shows that the probe has practically constant inductance in the entire frequency range due to the use of VF ferrite. The presence of a metal sample in the probe's magnetic circuit was manifested by a significant decrease in the inductance value at higher frequencies. In the case of the IN713LC + CrAl sample, an additional decrease in the value is evident, probably due to the structural inhomogeneity of the layer, which is caused by the increased Cr content. During measurement, the device determines the absolute value of the impedance and the phase angle from the complex impedance (Fig. 9 and Fig. 10). During the measurement, the influence of the thin layer was evaluated with respect to the reference state, which was the surface without a thin layer. The different properties of the IN713LC + CrAl layers are evident from the graphs, where the layer with IN713LC + Al shows significantly smaller

changes in impedance depending on the frequency, which indicates a better homogeneity of the coating.

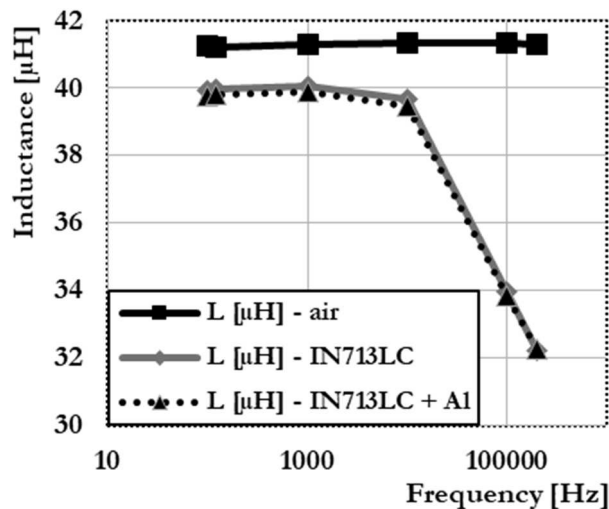


Fig. 7 Inductance of Inconel 713LC + Al

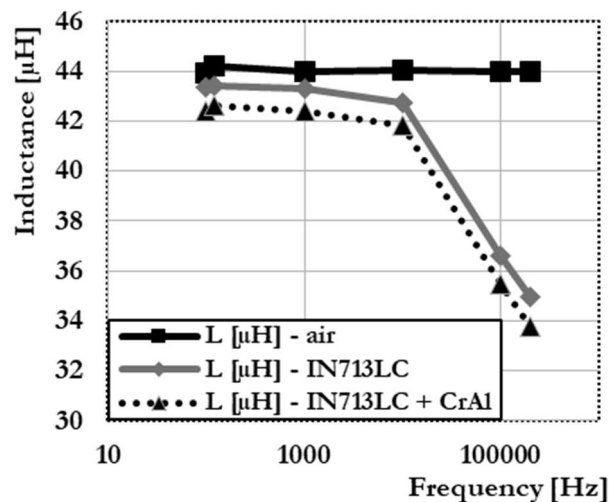


Fig. 8 Inductance of Inconel 713LC + CrAl

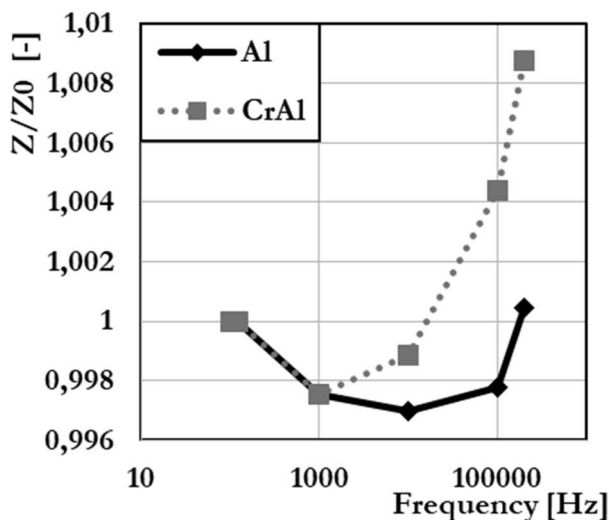


Fig. 9 Relative impedance change

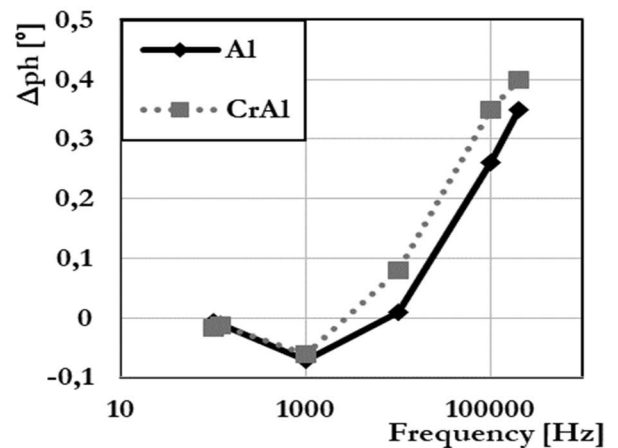


Fig. 10 Phase change  $\Delta\phi$

#### 4 Conclusions

Realized measurements in the presented article dealt with possibilities of using impedance spectroscopy for indirect measurements of thin layers of Al and Cr-Al coatings on Ni-based Inconel 713LC superalloy applied by the "Out-of-pack" diffusion method. Experimental measurements demonstrate the possibility of using impedance spectroscopy methods for research on measuring the thickness of thin layers based on Al and Cr. However, the measurements require precise measurement of impedance with an accuracy of  $1\text{m}\Omega$  and phase angle with an accuracy of  $0.001^\circ$  with high stability of the measuring frequency. For a better assessment of the parameters of the layers, it is necessary to extend the frequency range of the measurement to the range of MHz units, which will be the subject of future research.

#### Acknowledgement

*This work was supported by the Slovak Research and Development Agency under the contract No. SK-PL-21-0057: Study of resistance superalloys with/without coatings to high temperature oxidation; And also realized within the frame of the project Advancement and support of R&D for "Centre for diagnostics and quality testing of materials" in the domains of the RIS3 SK specialization, ITMS2014+: 313011W442, supported by the Operational Program Integrated Infrastructure financed through European Regional Development Fund.*

#### References

- [1] FURRER, D., FECHT H. (1999). Ni-based superalloys for turbine discs. In: JOM, Vol. 51, pp. 14-17.

- [2] KIANICOVÁ, M., KAFRÍK, J., TRNÍK, J. (2016). Degradation of aluminide coatings deposited on nickel superalloys. In: *Procedia Engineering*, Vol. 136, pp. 346–352.
- [3] WARNES, B.M., DUSHANE, N.S., COCKERILL, J.E. (2001). Cyclic oxidation of diffusion aluminide coatings on cobalt base super alloys. In: *Surface and Coatings Technology*, Vol. 148, No. 2-3, pp. 163-170.
- [4] POMEROY, M. J. (2005). Coatings for gas turbine materials and long term stability issues. In: *Materials & design*, Vol. 26. No. 3, pp. 223-231.
- [5] GOWARD, G. W. Progress in coatings for gas turbine airfoils. *Surface and coatings technology*, 1998, 108: 73-79.
- [6] LIN, R.Q., FU, C., LIU, M., et al. (2017). Microstructure and oxidation behavior of Al+Cr co-deposited coatings on nickelbased superalloys. In: *Surface and Coatings Technology*, Vol. 310, pp. 273–277.
- [7] ZAGULA-YAVORSKA, M., SIENIAWSKI, J. (2018). Cyclic oxidation of palladium modified and nonmodified aluminide coatings deposited on nickel base superalloys. In: *Archives of Civil and Mechanical Engineering*, Vol.18. No.1, pp. 130-139.
- [8] YANG, Y. F., et al. (2016). Effect of aluminisation characteristics on the microstructure of single phase  $\beta$ -(Ni, Pt) Al coating and the isothermal oxidation behaviour. In: *Corrosion Science*, Vol. 106, pp. 43-54.
- [9] ŠULÁK, I., et al. (2020). Low cycle fatigue and dwell-fatigue of diffusion coated superalloy Inconel 713LC at 800°C. In: *Materials Characterization*, Vol. 169, 110599.
- [10] ZANG, J., et al. (2016). Oxidation behaviour of the nickel-based superalloy DZ125 hot-dipped with Al coatings doped by Si. In: *Corrosion Science*, Vol. 112, pp. 170-179.
- [11] ESIN, V.A., et al. (2016). Increase in ductility of Pt-modified nickel aluminide coating with high temperature ageing. In: *Acta Materialia*, Vol. 105, pp. 505-518.
- [12] SAUCEDO-MORA, L., et al. (2015). Multi-scale modeling of damage development in a thermal barrier coating. In: *Surface and Coatings Technology*, Vol. 276, pp. 399-407.
- [13] LEYENS, C.; PINT, B. A.; WRIGHT, I. G. (2000). Effect of composition on the oxidation and hot corrosion resistance of NiAl doped with precious metals. In: *Surface and Coatings Technology*, Vol. 133, pp. 15-22.
- [14] GOWARD, G. W. (1998). Progress in coatings for gas turbine airfoils. In: *Surface and coatings technology*, Vol. 108, pp. 73-79.
- [15] WEI, L., GUO, L., LI, M., GUO, H. (2017). Calcium-magnesium-alumina-silicate (CMAS) resistant Ba<sub>2</sub>REAlO<sub>5</sub> (RE=Yb, Er, Dy) ceramics for thermal barrier coatings. In: *Journal of the European Ceramic Society* Vol. 37, pp. 4991–5000.
- [16] LI, X, et al. (2014). Effects of substrate material and TBC structure on the cyclic oxidation resistance of TBC systems. In: *Surface and Coatings Technology*, Vol. 258, pp. 49-61.
- [17] SALDAÑA, J. M., et al. (2018). Microstructure and lifetime of Hf or Zr doped sputtered NiAlCr bond coat/7YSZ EB-PVD TBC systems. In: *Surface and Coatings Technology*, Vol. 335, pp. 41-51.
- [18] OBRTLÍK, K, et al. (2017). Effect of alumina-silica-zirconia eutectic ceramic thermal barrier coating on the low cycle fatigue behaviour of cast polycrystalline nickel-based superalloy at 900° C. In: *Surface and Coatings Technology*, Vol. 318, pp. 374-381.
- [19] GODLEWSKI, K., GODLEWSKA, E. (1986). Effect of chromium on the protective properties of aluminide coatings. In: *Oxidation of metals*, Vol. 26, pp. 125-138.
- [20] JEDLINSKI, J., GODLEWSKI, K., MROWEC, S. (1989). The influence of implanted yttrium and cerium on the protective properties of a  $\beta$ -NiAl coating on a nickel-base superalloy. In: *Materials Science and Engineering: A*, Vol. 120, pp. 539-543.
- [21] DAS, D. K. (2013). Microstructure and high temperature oxidation behavior of Pt-modified aluminide bond coats on Ni-base superalloys. In: *Progress in Materials Science*, Vol. 58, No. 2, pp. 151-182.
- [22] DAI, P., et al. (2013). The effect of silicon on the oxidation behavior of NiAlHf coating system. In: *Applied surface science*, Vol. 271, pp. 311-316.
- [23] NICHOLLS, J. R. (2000). Designing oxidation-resistant coatings. In: *JoM*, Vol. 52, No. 1, pp. 28-35.
- [24] POKLUDA, J., KIANICOVÁ, M. (2010). Damage and performance assessment of protective coatings on turbine blades. In: *Gas*

- turbines, pp. 283–306, SCIYO, Rijeka; ISBN: 978-953-307-146-6.
- [25] POMEROY, M.J. (2005). Coatings for gas turbine materials and long term stability issues. In: *Materials & design*, Vol. 26, No. 3, pp. 223–231.
- [26] OKAZAKI, M. (2001). High-temperature strength of Ni-base superalloy coating. In: *Science and Technology of Advanced Materials*, Vol. 2, No. 2, pp. 357–366.
- [27] POURSAEIDI, et al. (2008). Failure analysis of a second stage blade in a gas turbine engine. In: *Engineering failure analysis*, Vol. 15, pp. 1111–1129.
- [28] ESKNER, M., SANDSTRÖM, R. (2003). Measurement of the ductile-to-brittle transition temperature in a nickel aluminide coating by a miniaturised disc bending test technique. In: *Surface and coatings technology*, Vol. 165, pp. 71–80.
- [29] CÍGER, R., BARÉNYI, I., KRBAŤA, M. (2021). Analysis of heat treatment parameters on the properties of selected tool steels M390 and M398 produced with powder metallurgy. In: *Manufacturing Technology*, Vol. 21, pp. 774–780.
- [30] MAJERÍK, J., MAJERSKÝ, J., BARÉNYI, I., CHOCHLÍKOVÁ, H., ESCHEROVÁ, J., KUBASÁKOVÁ, M. (2023). Surface Roughness, Topography, Accuracy, Chip Formation Analysis & Investigation of M390 and M398 Steels after Hard Machining. In: *Manufacturing Technology*, Vol. 23, pp. 60–72.
- [31] KLUČIAR, P., BARENYI, I., MAJERÍK, J. (2022). Nanoindentation Analysis of Inconel 625 Alloy Weld Overlay on 16Mo3 Steel. In: *Manufacturing Technology*, Vol. 22, pp. 26–33.
- [32] SKOCOVSKY, P., PODRABSKY, T., BELAN, J. (2004). Degradacja w wyniku eksploatacji warstwy aluminiowo-krzemowej łopatek turbinowych wykonywanych na bazie Ni. In: *Archiwum Technologii Maszyn i Automatyzacji*, Vol. 24, No. 1, pp. 45–52.